CrossMark

Selective electrode patterning of ITO films using pulsed ultraviolet laser

H. K. Lin[1] · **W. C. Hsu**[1] · **L. C. Tsao**[1]

Abstract　A method combining laser annealing and chemical etching is proposed for the selective patterning of indium tin oxide (ITO) films. ITO films with a thickness of 100 nm are deposited on glass using a radio frequency magnetron sputtering system. The as-deposited films have a transmittance of 75 % at a wavelength of 550 nm and a sheet resistance of 81 $\Omega/\square$. The ITO films are annealed using an ultraviolet (UV) laser system and are then immersed in oxalic acid etchant. It is found that the laser annealing process readily induces micro-cracks or voids in the ITO thin films, and therefore prompts electrical failure. However, through an appropriate specification of the scanning pitch, laser pulse energy and overlapping rate, the optoelectronic and crystalline properties can be significantly improved. Under the optimal annealing conditions, the transmittance is increased to 82 % and the sheet resistivity is reduced to 50 $\Omega/\square$. Notably, the surface roughness of the corresponding etched sample is just 1.5 nm, while the residual stress is equal to 417 MPa.

✉　H. K. Lin
　　hsuankai@msn.com; HKLin@mail.npust.edu.tw

[1]　Graduate Institute of Materials Engineering, National Pingtung University of Science and Technology, Pingtung 912, Taiwan R.O.C.

Published online: 16 January 2016

🍃 Springer

1 Introduction

Indium tin oxide (ITO) has low electrical resistance and high optical transparency in the visible range. As a result, it is used as an electrode material in many applications nowadays, including flat panel displays and solar cells (Betz and Kharrazi 2006; Guillén and Herrero 2011; Bu 2014). ITO films are generally patterned using a photolithography technique and then furnace annealed at temperatures in excess of 200 °C in order to obtain a crystalline structure (Morikawa and Fujita 2000). However, such an approach is not only expensive, but may also cause substrate damage. As a result, the direct laser patterning of ITO electrodes has gained increasing interest in recent years (Yavas et al. 1999; Rung et al. 2014; Abreu et al. 2013; Risch and Hellmann 2011; Solieman et al. 2010). The quality of ablated ITO films is significantly dependent on the processing parameters. For example, grooves with well defined features can be obtained on the ITO surface by using a shorter pulse duration and a shorter laser wavelength (Yavas et al. 1999).

In patterning ITO films, the ablation process requires sufficient energy to melt and evaporate the materials. However, an excessive energy input may damage the substrate as a result of thermally-induced stress. Moreover, for devices which are fabricated directly on the substrate, a high energy input may result in the melting and subsequent resolidification of excess material along the edge of the ablation trench; leading to a loss in pattern definition. Accordingly, the feasibility of patterning ITO films using a two-step process combining laser annealing followed by chemical etching has attracted growing attention recently (Cheng et al. 2010). In such an approach, the ITO film is first patterned using low laser irradiation, thereby prompting a transition of the ablated material to a crystalline phase. The patterned film is then immersed in an etchant solution, resulting in the differential removal of the amorphous and crystalline regions of the film, respectively. However, in the patterning stage of the process, the pulse repetition rate must be carefully controlled so as to prevent crack formation in the ITO film and subsequent electrical failure (Lee et al. 2012). Previous studies have suggested that the optical and electrical properties of ITO films can be enhanced by performing the patterning process using a femtosecond laser (Cheng and Lin 2014).

This study performs an experimental investigation into the optimal values of the pulse energy, scanning pitch and scanning speed for a two-stage ITO patterning process comprising UV laser irradiation followed by chemical etching. The effects of the annealing conditions on the electrical, optical and structural properties of the ITO thin films are evaluated. In general, the results suggest that a scanning pitch of 2 μm, a laser pulse energy of 1.5 μJ, and an overlapping rate of 99.9 % represent the optimal processing conditions for the present ITO thin films.

2 Experimental

Indium tin oxide thin films with a thickness of 100 nm were deposited on glass substrates using a RF magnetron sputtering system with an In_2O_3 (90 wt%):SnO_2 (10 wt%) target. Note that full details of the deposition process are provided in a previous study by the present group (Lee et al. 2012). The as-deposited films were annealed using a UV laser (Coherent AVIA 355-7000) with a wavelength of 355 nm and a focused spot size of 16 μm. In order to identify the optimal processing conditions, the ablation process was performed using various pulse repetition rates in the range of 55–70 kHz, scanning pitch distances in the range of 2–8 μm, and laser scanning speeds in the range of 0.5–100 mm/s. Following the annealing process, the ITO films were immersed in 0.05 M oxalic acid etchant for 4 min.

The pulse energy (E) in the annealing process is given by (Benware et al. 1998)

$$E = P_{AVG}/rep, \tag{1}$$

where P_{AVG} and rep denote the average power of the pulse laser and the repetition rate, respectively. For the ablation trials performed in the present study, the pulse energy had values of 1.28–1.64 μJ for the considered repetition rates of 70–55 kHz.

According to (Choi et al. 2007; Sabbaghzadeh et al. 2008), the overlapping rate during laser annealing is given by

$$O_f = \left(1 - \frac{v/f}{D + vt}\right) \times 100, \tag{2}$$

where D is the spot size of the laser beam, t is the pulse duration, f is the pulse frequency, and v is the scanning speed. In the present trials, the overlapping rate was equal to 89.5, 94.7, 98.9, 99.4 and 99.9 % (for scanning speeds of 100, 50, 10, 5 and 0.5 mm/s, respectively).

The surface morphologies of the various samples were examined using a field emission scanning electron microscope (FESEM, JSM-7600F) and an atomic force microscope (AFM, CP-II). Conventional XRD studies on the films were carried out using a diffractometer (Bruker D8) with Cu-Kα radiation. The sheet resistance was measured using a four-point probe method. The optical transmittance was measured using a UV-VIS-IR spectrophotometer (Lambda 35). Finally, the residual stress was evaluated using the conventional $\sin^2\Psi$ method (Ma et al. 2002).

3 Results and discussion

The sheet resistivity and optical transmittance of the as-deposited thin films were found to be 81 Ω/□ and 75 % at 550 nm, respectively. Figure 1 shows the variation of the sheet resistance with the scanning pitch before and after the annealing process given a pulse repetition rate of 60 kHz, a scanning speed of 5 mm/s and a pulse energy of 1.5 μJ. As
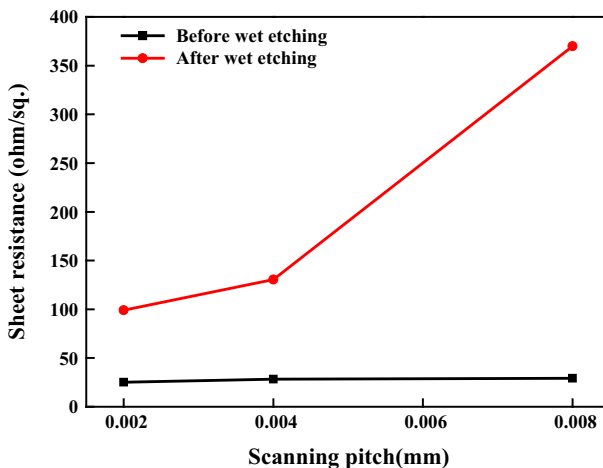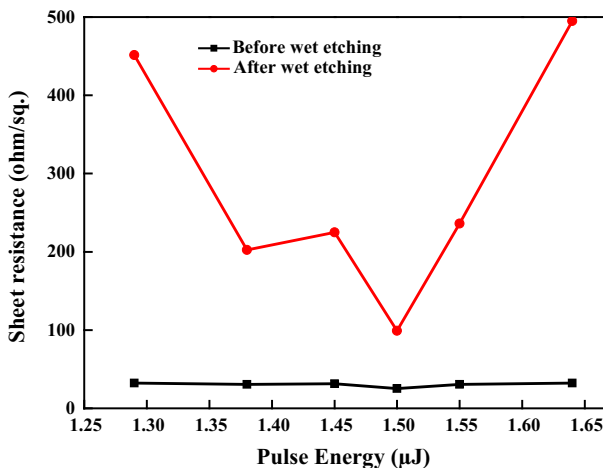

Fig. 1 Variation of sheet resistance with scanning pitch for annealed and etched samples

shown, the sheet resistance reduces from 81 $\Omega/\square$ in the as-deposited condition to 25 $\Omega/\square$ following the laser annealing process. The improvement in the sheet resistance can be attributed to the enhanced mobility of the carriers in the annealed samples (Coutts et al. 2000; Morikawa and Fujita 2000). The sheet resistance of the annealed films is insensitive to the scanning pitch. However, the resistance increases significantly following chemical etching; particularly in the samples annealed using a higher scanning pitch. Overall, the results imply that the scanning pitch has an optimal value of 2 μm for the present ITO samples. Figure 2 shows the sheet resistance of the etched and non-etched samples annealed with a scanning pitch of 2 μm and a pulse energy in the range of 1.28–1.64 μJ. It is seen that for the as-annealed samples, the sheet resistance has a constant value of around 30 $\Omega/\square$, irrespective of the pulse energy. However, following the etching process, the sheet resistance increases. For example, in the samples annealed with pulse energies of 1.28–1.64 μJ, the sheet resistance increases to 451–495 $\Omega/\square$, respectively. Of the various samples, the minimum value of the sheet resistance is obtained in the sample annealed with a pulse energy of 1.5 μJ. Figure 3 shows the sheet resistance of the samples annealed with a scanning pitch of 2 μm, a laser pulse energy of 1.5 μJ and overlapping rates ranging from 89.5 to 99.9 %. The results show that the sheet resistance of the annealed films is insensitive to the overlapping rate, but increases following chemical etching. Moreover, for the etched films, the sheet resistance decreases for overlapping rates greater than 94.7 %. For example, given the maximum overlapping rate of 99.9 %, the sheet resistance falls to around 50 $\Omega/\square$.

Figure 4a, b show the optical transmittance of the annealed ITO films before and after chemical etching, respectively. An inspection of Fig. 4a shows that the transmittance of the as-deposited ITO film (75 % at a wavelength of 550 nm) increases to 82 % after the annealing process. Moreover, observing both figures, it is seen that the annealed samples have good optical transparency in both the etched and the non-etched conditions. Figure 5a, b show the XRD patterns of the various ITO samples before and after chemical etching, respectively. Figure 5a shows that the XRD pattern of the as-deposited ITO film has no prominent peaks. Hence, it is inferred that the film has an amorphous structure. However, following annealing, the spectra exhibit peaks at the (222), (400), (440) and
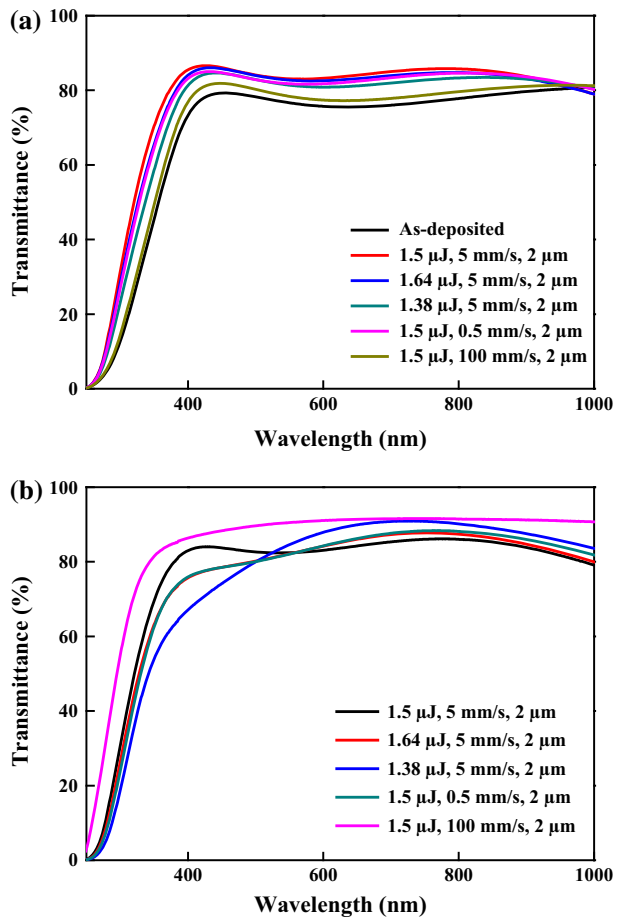

Fig. 2 Variation of sheet resistance with pulse energy for annealed and etched samples
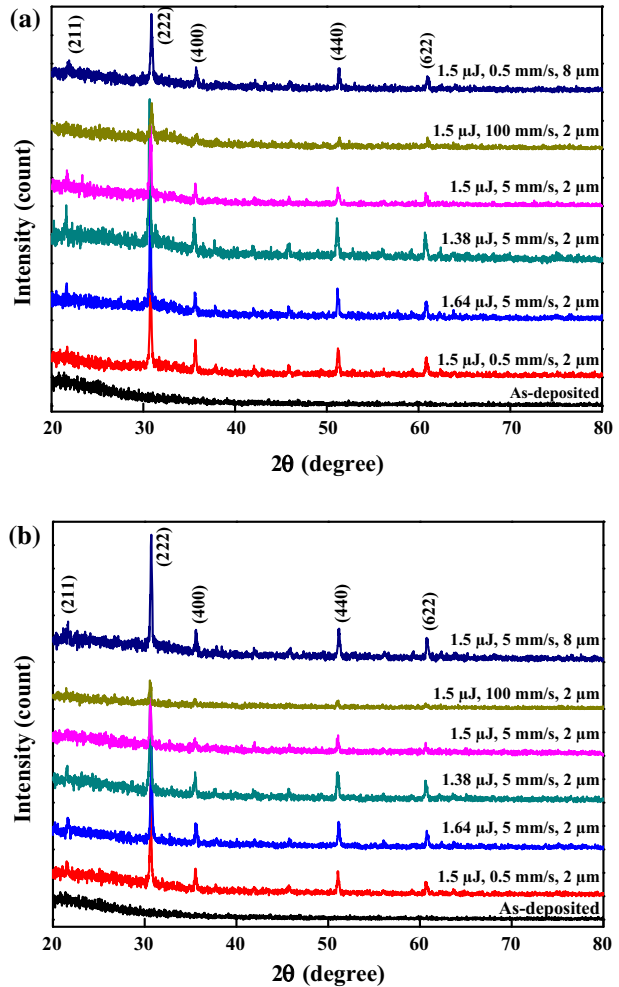
Fig. 3 Variation of sheet resistance with overlapping rate for annealed and etched samples
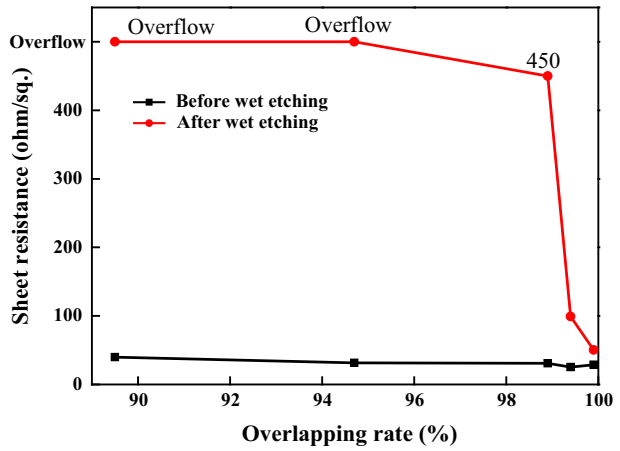
Fig. 4 Optical transmittance spectra of as-deposited and annealed ITO samples: **a** before and **b** after wet etching process

Fig. 5 XRD spectra of as-deposited and annealed ITO samples: **a** before and **b** after wet etching process


(622) planes, which indicates that the films have a polycrystalline state. Figure 5b confirms that the polycrystalline structure is retained following the etching process. In both figures, the peaks in the XRD spectrum of the sample annealed with a scanning speed of 100 mm/s have a lower intensity than those in the spectra of the other samples. Thus, the results suggest that a slower scanning speed results in a more crystalline property.

Figure 6a, b present SEM images of the samples annealed at scanning speeds of 100–0.5 mm/s, respectively. It is seen that the sample annealed at a scanning speed of 0.5 mm/s contains a greater number of crystalline grains than that annealed at 100 mm/s. In other words, the crystalline property of the annealed samples increases as the local input thermal energy increases (i.e., the overlapping ratio increases). Figure 7 presents SEM images of the films following the chemical etching process. As shown in Fig. 7d, the sample annealed with a scanning speed of 0.5 mm/s retains a small and uniform grain size and has well defined grain boundaries. However, the surfaces of the remaining samples contain a large number of voids and micro-cracks. Thus, it is inferred that under the
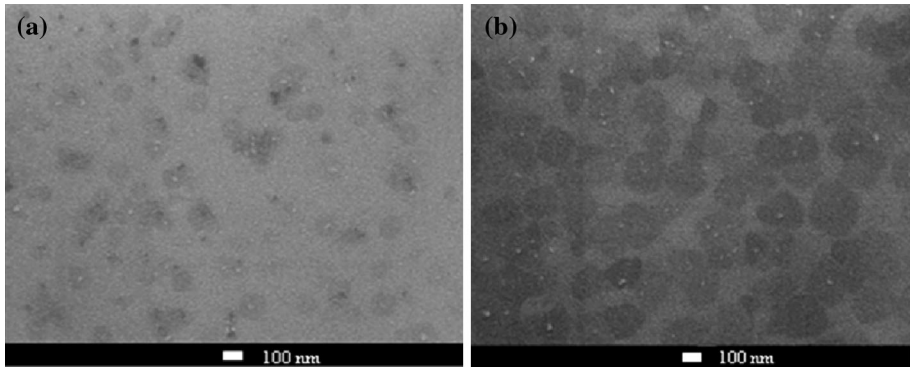
Fig. 6 SEM images of non-etched ITO samples annealed with laser parameters of: **a** 100 mm/s and **b** 0.5 mm/s
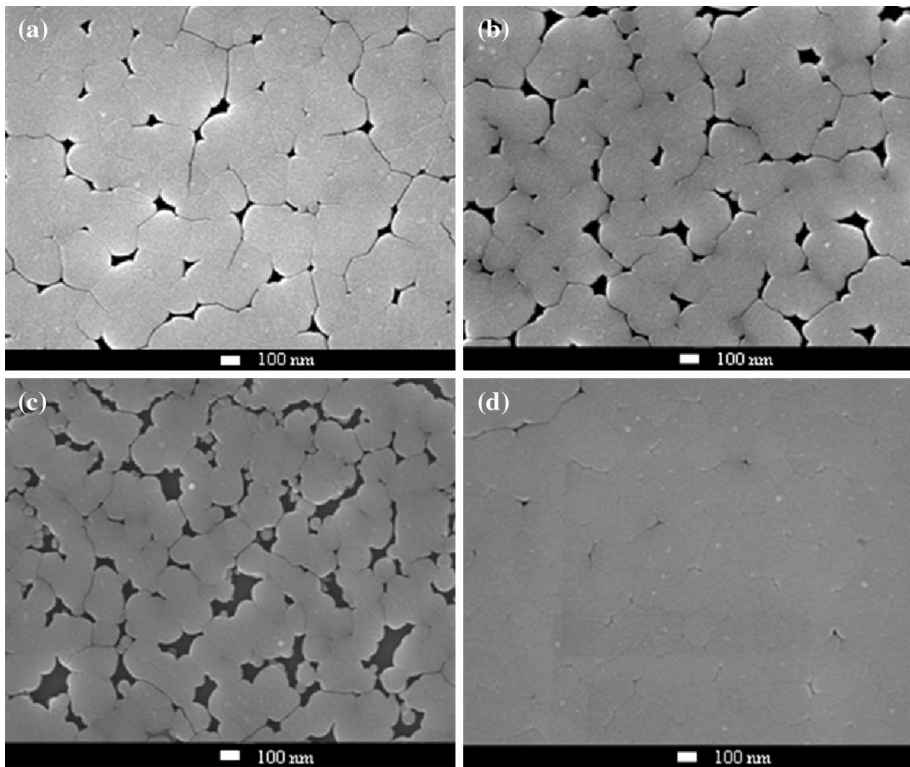
Fig. 7 SEM images of etched ITO samples annealed with laser parameters of: **a** 1.64 μJ, **b** 1.38 μJ, **c** 100 mm/s and **d** 0.5 mm/s

processing conditions shown in Fig. 7a, c, the energy supplied to the ITO thin film during the annealing process results in the formation of defects, which prompt surface cracking in the subsequent etching process. It is noted that the micro-crack tendencies of the samples

shown in Fig. 7a, d are consistent with the sheet resistance results presented in Figs. 1, 2 and 3. In other words, the presence of micro-cracks in the sample surface leads to a higher sheet resistance.

Figure 8 shows the sheet resistance of the etched ITO samples as a function of the scanning speed and pulse energy. As shown, the figure comprises three distinct regions. In the first region, the samples have a poor crystal quality and contain many defects following the etching process. Consequently, an overflow of the sheet resistance occurs. In the second region, the samples contain a lesser number of voids following the chemical etching process (see Fig. 7). However, the presence of these voids still leads to a high sheet resistance (85–700 $\Omega/\square$). Finally, in the third region, characterized by low scanning speeds (i.e., <5 mm/s) and pulse energies in the range of 1.45–1.55 μJ, the etched samples have good crystalline properties, and thus have a low sheet resistance of approximately 50 $\Omega/\square$.

Figure 9 show the surface roughness values before and after etching for ITO thin films annealed with laser energies in the range of 1.38–1.64 μJ and a constant scanning speed of 5 mm/s. The as-deposited ITO film has a roughness of 4.8 nm. However, for the annealed ITO films, the surface roughness is less than 2.9 nm and reduces as the laser energy decreases. Following the etching process, the surface roughness of the annealed samples has a constant value of around 1.5 nm, irrespective of the laser pulse energy used in the annealing process. Figure 10 shows the variation of the surface roughness with the scanning speed for the etched and non-etched samples. It is observed that the surface roughness increases from around 1.8 to 2.8 nm following the etching process given a laser scanning speed higher than 30 mm/s. By contrast, for scanning speeds of less than 30 mm/s, the surface roughness of the etched films is less than that of the corresponding un-etched samples. In other words, it is inferred that a higher overlapping rate is beneficial in reducing the surface roughness of the annealed films following chemical etching.

The residual stress in the ITO films was measured using the conventional $\sin^2\Psi$ method. Figure 11 plots the variation of $(d-d_o)/d_o$ with $\cos^2\alpha \sin^2\Psi$ for the etched samples annealed with a pulse energy of 1.5 μJ, a scanning pitch of 2 μm, and scanning speeds of 0.5–5 mm/s, respectively. Note that in obtaining the results, α was maintained at a constant value of $\alpha = \theta o - \gamma$, Ψ was varied in the range of 0°–54.2°, and d_o (the initial lattice space) was
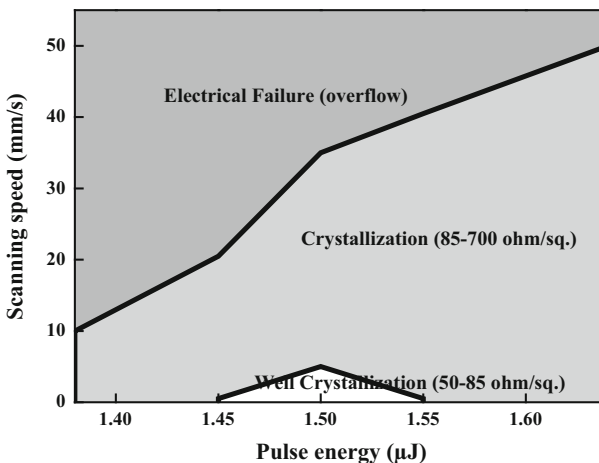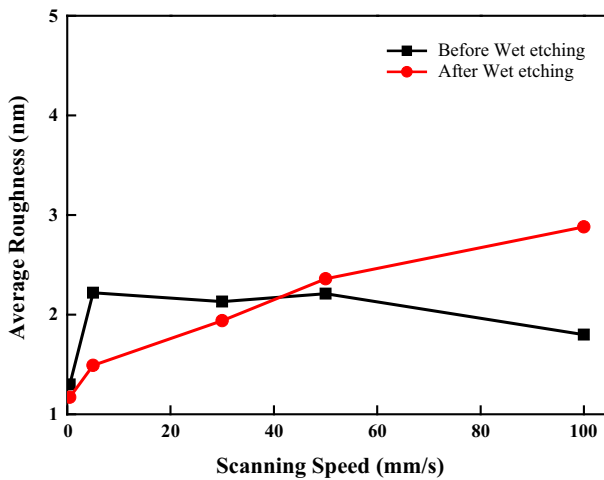

Fig. 8 Sheet resistance of etched ITO samples as function of scanning speed and pulse energy
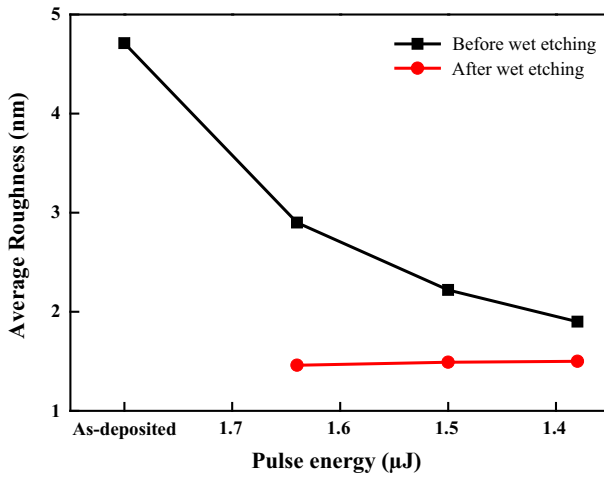
Fig. 9 Variation of surface roughness with pulse energy for annealed and etched samples

Fig. 10 Variation of surface roughness with scanning speed for annealed and etched samples

assumed to be ~ 0.152 nm). Finally, the diffraction peak was located at $60.7°$ and the incident angle was set as $1°$. The gradients of the fitted slopes for the samples annealed at scanning speeds of 0.5–5 mm/s have values of 0.00344 and 0.00359, respectively. The residual stress of the two specimens can be calculated using the slope equaling function $((1 + \nu)/E)\sigma$, where ν and E are the Poisson ratio (~ 0.33) and Young's modulus (~ 160 GPa) of ITO, respectively. Therefore, the residual stress of the specimen annealed at a scanning speed of 0.5 mm/s is equal to 417 MPa, while that of the specimen annealed at a scanning speed of 5 mm/s is equal to 432 MPa. In other words, the residual stress reduces with an increasing overlapping rate. In general, the propensity of annealed films toward cracking following etching reduces as the residual stress reduces. Moreover, the properties of ITO thin films improve given a residual stress of less than 420 MPa (Lin and Hsu 2014),
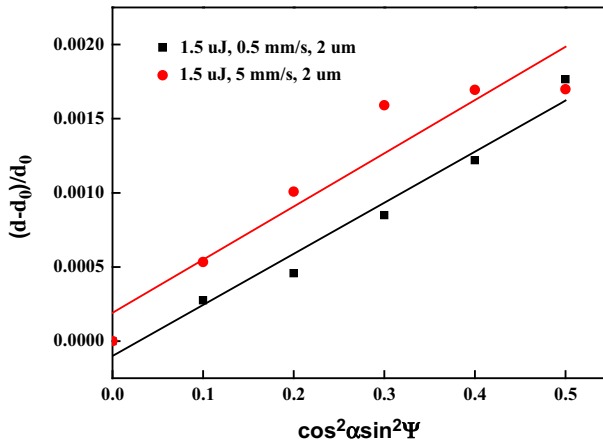
Fig. 11 Variation of (d–do)/do with $\cos^2\alpha \sin^2\Psi$ for the annealed and etched samples annealed with laser scanning speeds of 0.5–5 mm/s

Thus, the results presented in Fig. 11 suggest that a scanning speed of 0.5 mm/s (i.e., an overlapping ratio of 99.9 %) represents the optimal scanning speed for the present specimens.

4 Conclusions

ITO films deposited on glass substrates were patterned as electrodes using a laser annealing process followed by chemical etching. Laser processing was performed using a 355 nm laser, a scanning pitch in the range of 2–8 μm, a pulse energy in the range of 1.3–1.64 μJ, and a scanning speed in the range of 0.5–100 mm/s. The results have shown that the samples annealed with a higher scanning pitch (8 μm), higher pulse energy (1.64 μJ), and lower overlapping rate (~ 89 %) contain many surface voids and micro-cracks following the etching process, and therefore have a high sheet resistance. However, given an appropriate setting of the annealing parameters, ITO films with good crystalline properties can be obtained. For the present laser source, the optimal processing parameters include a scanning pitch of 2 μm, a pulse energy of 1.5 μJ, and an overlapping rate of ~ 99.9 %. Given these parameter settings, micro-cracking of the etched samples is suppressed, and hence ITO films with a low sheet resistance, high optical transmittance, low surface roughness and low residual stress are obtained.

References

Abreu Fernandes, S., Schoeps, B., Kowalick, K., Nett, R., Esen, C., Pickshaus, M., Ostendorf, A.: Femtosecond laser ablation of ITO/ZnO for thin film solar cells. Phys. Procedia **41**, 795–802 (2013)

🖉 Springer

Benware, B.R., Macchietto, C.D., Moreno, C.H., Rocca, J.J.: Demonstration of a high average power tabletop soft X-ray laser. Phys. Rev. Lett. **81**, 5804–5807 (1998)

Betz, U., Olsson, M.K., Marthy, J., Escolá, M.F., Atamny, F.: Thin films engineering of indium tin oxide: large area flat panel displays application. Surf. Coat. Technol. **200**, 5751–5759 (2006)

Bu, I.Y.Y.: A simple annealing process to obtain highly transparent and conductive indium doped tin oxide for dye-sensitized solar cells. Ceram. Int. **40**, 3445–3451 (2014)

Cheng, C.-W., Lin, C.-Y.: High precision patterning of ITO using femtosecond laser annealing process. Appl. Surf. Sci. **314**, 215–220 (2014)

Cheng, C.-W., Chen, J.-S., Chen, H.-H.: Patterning of crystalline ITO using infrared nanosecond fiber laser pulses. Mater. Manuf. Process. **25**, 684–688 (2010)

Choi, H.W., Farson, D.F., Bovatsek, J., Arai, A., Ashkenasi, D.: Direct-write patterning of indium-tin-oxide film by high pulse repetition frequency femtosecond laser ablation. Appl. Opt. **46**, 5792–5799 (2007)

Coutts, T.J., Young, D.L., Li, X.: Characterization of transparent conducting oxides. MRS Bull. **25**, 58–65 (2000)

Guillén, C., Herrero, J.: TCO/metal/TCO structures for energy and flexible electronics. Thin Solid Films **520**, 1–17 (2011)

Lee, C.J., Lin, H.K., Li, C.H., Chen, L.X., Lee, C.C., Wu, C.W., Huang, J.C.: A study on electric properties for pulse laser annealing of ITO film after wet etching. Thin Solid Films **522**, 330–335 (2012)

Lin, H.K., Hsu, W.C.: Electrode patterning of ITO thin films by high repetition rate fiber laser. Appl. Surf. Sci. **308**, 58–62 (2014)

Ma, C.H., Huang, J.H., Chen, H.: Residual stress measurement in textured thin film by grazing-incidence X-ray diffraction. Thin Solid Films **418**, 73–78 (2002)

Morikawa, H., Fujita, M.: Crystallization and electrical property change on the annealing of amorphous indium-oxide and indium-tin-oxide thin films. Thin Solid Films **359**, 61–67 (2000)

Risch, A., Hellmann, R.: Picosecond laser patterning of ITO thin films. Phys. Procedia **12**, 133–140 (2011)

Rung, S., Christiansen, A., Hellmann, R.: Influence of film thickness on laser ablation threshold of transparent conducting oxide thin-films. Appl. Surf. Sci. **305**, 347–351 (2014)

Sabbaghzadeh, J., Hamedi, M.J., Ghaini, F.M., Torkamany, M.J.: Effect of process parameters on the melting ratio in overlap pulsed laser welding. Metall. Mat. Trans. B **39**, 340–347 (2008)

Solieman, A., Moharram, A.H., Aegerter, M.A.: Patterning of nanoparticulate transparent conductive ITO films using UV light irradiation and UV laser beam writing. Appl. Surf. Sci. **256**, 1925–1929 (2010)

Yavas, O., Ochiai, C., Takai, M.: Substrate-assisted laser patterning of indium tin oxide thin films. Appl. Phys. A **69**, S875–S878 (1999)